0031-3998/06/5903-0428
PEDIATRIC RESEARCH
Vol. 59, No. 3, 2006
Printed in U.S.A.

Maternal Exposure to LPS Induces Hypomyelination in the Internal Capsule and Programmed Cell Death in the Deep Gray Matter in Newborn Rats

CATHERINE I. ROUSSET, SYLVIE CHALON, SYLVAIN CANTAGREL, SYLVIE BODARD, CHRISTIAN ANDRES, PIERRE GRESSENS, AND ELIE SALIBA

INSERM U619 [C.I.R., S.Ch., S.Ca., S.B., C.A., E.S.], 37000 Tours, France; Universite François Rabelais de Tours [C.I.R., S.Ch., S.Ca., S.B., C.A., E.S.), 37000 Tours, France; INSERM U676 [P.G.], Hopital Robert-Debré, 75019 Paris, France

ABSTRACT: Epidemiologic and experimental findings implicate maternal infection in the etiology of injury to brain white matter, which may lead to cerebral palsy in preterm newborns. In the present study, inflammation and brain damage in 1- and 7-d-old rats were investigated after maternal inflammation. Intraperitoneal injection of 300 μg/kg of *Escherichia coli* lipopolysaccharide was administered to pregnant Wistar rats at d 19 and 20 of gestation (LPS group). Control females received a saline injection. Proinflammatory cytokines IL-1β, tumor necrosis factor-α, and IL-6 expression in the fetal brain were determined by reverse transcription quantitative polymerase chain reaction. Brain injury was examined in 16-μm coronal brain sections by GFAP, MBP, caspase-3 immunohistochemistry, and terminal deoxynucleotidyl transferase-mediated dUTP nick-end labeling. Expression of IL-1β was significantly increased 3 d after maternal administration (P1). A significant increase in cell death occurred at P1 and P7 in specific brain areas, *i.e.* in the subventricular striatal zone at P1, and in 1) the periventricular striatum, 2) the periventricular white matter, and 3) the germinative ventricular zone at P7. We also observed typical astrogliosis and strong hypomyelination in the external and internal capsule in the LPS group at P7. These results demonstrate that maternal LPS treatment induces persistent fetal inflammatory reactions associated with significant white matter injury in progeny at P1 and P7. This model should be relevant for the study of the pathophysiological mechanisms involved in cerebral white matter damage in preterm human newborns and in the development of therapeutic strategies. **(*Pediatr Res* 59: 428–433, 2006)**

The neuropathology of PVL consists of two main components, *i.e.* focal and diffuse (1,2). It is characterized by necrosis of the periventricular WM combined with more diffuse injuries. It is one of the most important lesions that occurs in the immature brain and results in life-long disorders of movement, posture, and cognition. Hypoxia-ischemia is known to be one of the causes of PVL, but maternal infection and inflammation are suggested as other important factors involved in the development of such lesions (3,4). The maternal immune response following infection may become deleterious for the fetus. Excessive secretion of cytokines is cytotoxic for the fetus and may induce fetal inflammatory response syndrome (5), which leads to astrogliosis, acts on oligodendrocytes during their maturation (6,7) and contributes to neonatal brain injury and later developmental disability (8).

Cytokines are signaling proteins that are produced as part of the inflammatory response. IL-1β expression in the brain is markedly increased after injury (9). In the human preterm infant, increased concentrations of proinflammatory cytokine IL-6, IL-1β, and TNF-α in neonatal blood, amniotic fluid, umbilical cord, or CSF have been associated with PVL and later impairment of neurodevelopment (10–12).

LPS is the bacterial cell wall of Gram-negative bacteria and is responsible for most of the inflammatory effects of infection due to bacteria. It has also been reported that LPS induces production of TNF-α and IL-1β (13). Significant WM lesions have been described in young dogs aged 1–10 d after injection of *Escherichia coli* (14). Peripheral and central injections of LPS have been shown to induce IL-1β bioactivity in the brains of laboratory animals, especially in rats (15).

Several animal models have been used to understand the consequences of maternal infection on offspring. Recent studies in rabbits have provided consistent results showing that maternal intrauterine infection with *E. coli* induces WM damage in fetal brains and cell death (16). After maternal injection of *E. coli* LPS at gestational d 18 (G18) and G19 in pregnant rats, hypomyelinization and increase in astrocytes were observed in 8-d-old pup brains (17). This study also described a dose-dependent peak of IL-1β and TNF-α mRNA expression in fetal rat brains at 1, 4, and 24 h after maternal injection at G18. Increase in cell death and expression of proinflammatory cytokines in the brain were observed only during the fetal period or a few hours after bacterial or LPS injection. It would therefore be very interesting to find out whether these processes are limited to the prenatal period or continue after birth

Received July 27, 2005; accepted October 10, 2005.
Correspondence: Elie Saliba, M.D., Ph.D., Service Medecine Néonatale, Hôpital Clocheville, 49 bd Béranger, 37044 Tours Cedex, France; e-mail: saliba@med.univ-tours.fr
This work was supported by INSERM and Region Centre, France.

DOI: 10.1203/01.pdr.0000199905.08848.55

Abbreviations: CSF, cerebrospinal fluid; **LPS,** lipopolysaccharide; **NO,** nitric oxide; **PCD,** programmed cell death; **PVL,** periventricular leukomalacia; **RT-QPCR,** reverse transcriptase quantitative polymerase chain reaction; **TNF,** tumor necrosis factor; **TUNEL,** terminal deoxynucleotidyl transferase-mediated dUTP nick-end labeling; **WM,** white matter

and thus might predispose the immature brain to postnatal lesions.

The purpose of this study was to determine the occurrence of delayed cell death, persistent cytokine expression, and WM injury in the brains of 1- (P1) and 7- (P7) day-old rats after maternal administration of *E. coli* LPS. This narrow window in rats corresponds to a large window in humans and represents a strong vulnerability window during brain development, especially in terms of oligodendrogenesis.

MATERIALS AND METHODS

Animals and drugs. Experiments on rats were carried out in compliance with European Community Commission directive guidelines (86/609/EEC). Time-pregnant Wistar rats used in this study were purchased from CERJ (Le Genest, France). They had free access to food and water and were bred at 22°C with a normal light cycle. Doses of 300 μg/kg (LPS group) of LPS (*E. coli*, serotype 055:B5; Sigma Chemical Co., St. Louis, MO), diluted in saline solution, were injected intraperitoneally to pregnant rats at 19 and 20 d of gestation. The control group consisted of pregnant rats injected with saline solution on the same days.

Newborn rats were killed at P1 and P7. We choose to study animals at P1 and P7 because these stages are equivalent to 22 and 36 wk of gestation in humans (18). Brains were dissected on ice, frozen in isopentane cooled to –35°C with dry ice, and stored at –80°C until use. Coronal sections of 16-μm thickness were prepared at –20°C in a cryostat microtome (Jung CM3000, Leica, Wetzlar, Germany), mounted on Superfrost slides and stored at –80°C until use. At P1, sections were taken from brain regions corresponding to plates 6, 7, 12, and 13 of Altman and Bayer's atlas (19). At P7, sections were taken from brain regions corresponding to plates 12, 13, 30, and 31 of Paxinos and Watson's atlas (20).

A total of 25 litters was used, 10 for controls and 15 for the LPS group. In the first group of six litters (two controls and four LPS group), pups were killed at P7. Two animals from each dam were used for histologic and TUNEL studies, and the rest were used for RT-PCR (22 controls and 24 LPS group). In the second group of 11 dams (4 controls and 7 LPS group), 4 animals from each dam were used at P7 for physiologic study and 7 pups from 4 control dams and 8 pups from 4 LPS group dams were used for immunohistochemistry. The rest were used at P1 (24 pups as controls and 36 pups from the LPS group) for physiologic study and RT-PCR. Finally, in the third group of 8 dams (4 controls and 4 LPS group), 2 pups from each were used for immunohistochemistry study at P1.

RT-QPCR. All chemicals and the oligonucleotide primers were purchased from Invitrogen (Carlsbad, CA). Total mRNA samples were extracted from brains using TRIzol reagent according to the manufacturer's instruction. After treatment with deoxyribonuclease I amplification grade, 1 μg RNA from each brain was reverse transcribed into cDNA by Superscript II reverse transcriptase (10 U/μL) with 0.5 mM dNTP mix and random hexamers (5 ng/μL). The reaction was performed on a thermocycler (iCycler, Bio-Rad, Hemel Hempstead, UK) at 65°C for 5 min, 45°C for 50 min, and termination at 70°C for 15 min.

Specific cDNA samples were amplified by PCR and oligonucleotide primer pairs designed for targeting IL-1β, IL-6, and TNF-α cDNA. For IL-1β and TNF-α, the reaction was performed in 25 μL of final volume, containing 12.5 μL of 2× platinum SYBR green qPCR Supermix UDG, 15 μM of each primer, 4 μL of cDNA from the RT mix, and H_2O added to achieve the final volume. The PCR reaction conditions were 2 min at 50°C, 40 cycles at 95°C for 20 s, 60°C for 40 s, 84°C for 10 s. For IL-6, the PCR reaction was performed in 25 μL of final volume, consisting of 2.5 μL of 10× PCR buffer, 1.5 mM magnesium chloride, 0.125 mM dNTP, 0.5 μM of each primer, 4 μL of cDNA, 0.07 U/μL of *Taq*DNA polymerase, 0.2× of SYBR green and H_2O added to achieve the final volume. The PCR reaction conditions were 3 min at 94°C, 40 cycles at 94°C for 30 s, 62°C for 30 s, 72°C for 30 s, 82°C for 10 s. For all genes, a melting curve from 72 to 94°C was performed at the end of the reaction to verify the nature and purity of the PCR products. Since β-actin was used as control, the PCR reaction was the same as the target gene. The sequences for the primer pairs are listed in Table 1. We used the $2^{\Delta\Delta CT}$ method to make comparisons where $\Delta C_T = (C_{Ttarget} - C_{TActin})$, and $\Delta\Delta C_T = \Delta C_{T\ controls} - \Delta C_{T\ LPS\ group}$ (21). Threshold cycle values of two replicates from each sample were averaged. We considered that the difference between the threshold cycle of the two replicates should be <0.5 to be usable. The ratio (target cDNA)/(β-actin cDNA) was calculated to normalize the target cDNA values.

Table 1. *Primers used for RT-qPCR and the size of the amplified fragments*

IL-1β	199 bp	5′-TGA AGC AGC TAT GGC AAC TG-3′ (sense)
		5′-TGC CTT CCT GAA GCT CTT GT-3′ (antisense)
TNF-α	188 bp	5′-TGA TCC GAG ATG TGG AAC TG-3′ (sense)
		5′-GAG CCC ATT TGG GAA CTT CT-3′ (antisense)
IL-6	191 bp	5′-AGT TGC CTT CTT GGG ACT GA-3′ (sense)
		5′-CAG AAT TGC CAT TGC ACA AC-3′ (antisense)
β-actin	143 bp	5′-GCC CTA GAC TTC GAG CAA GA-3′ (sense)
		5′-AGG AAG GAA GGC TGG AAG AG-3′ (antisense)

Cresyl violet staining. After immersion in cresyl violet, slides were rinsed and dehydrated by immersion in baths of increasing concentrations of ethanol. After baths in Histo-Clear, slides were mounted with counter-staining. Four sections from each cerebral region and each brain were examined under microscope to detect histologic changes.

Caspase-3 immunohistochemistry. Anti-rabbit caspase-3 (Ozyme, St. Quentin Yvelines Cedex, France) were used as primary antibodies for detection of cell death and EnVision Kit (DAKO, Copenhagen, Denmark) for visualization. Sections were fixed for 3 min in methanol, 4 min in acetone, dried for 30 min, heated in citrate buffer (8.2 mM Na citrate and 1.8 mM citric acid, pH 6) in a microwave for 10 min and rinsed. Sections were incubated for 5 min in Peroxidase block solution, rinsed and incubated with primary antibody diluted 1:200 in Tris buffer saline (TBS; 50 mM Trizma, 150 mM NaCl, and 0.05% Tween 20, Sigma Chemical Co.) overnight. After rinsing with TBS, sections were incubated with peroxidase polymer for 30 min. After washing in TBS, sections were stained with 3,3′-diaminobenzidine and mounted with counter-staining.

TUNEL. Sections were fixed with 4% PFA (paraformaldehyde) bath for 15 min, rinsed in 0.1 M PBS (50 mM of disodium hydrogen phosphate and 200 mM of dihydrogen phosphate sodium, pH 7.4), and dehydrated by immersion in baths of increasing concentrations of ethanol. Sections were digested in 1 μg/mL proteinase K for 10 min and rinsed in PBS. After endogenous peroxidase inhibition by 10 min incubation in 2% H_2O_2, sections were rinsed in PBS and incubated 1 h at 37°C with biotin-dUTP (25 μL per section: 5 μL of 5× terminal deoxynucleotidyl transferase (Tdt) buffer, 0.2 μL Tdt enzyme, 0.15 μL biotin-16-2′-deoxyuridine-5′-triphosphate, and H_2O added to achieve final volume). After washing in PBS, sections were incubated with 2% BSA for 30 min, rinsed in PBS and incubated for 30 min with the avidin-biotin-peroxidase complex (Vectastain ABC kit, Vector Laboratories, Burlingame, CA). Finally, sections were stained with 3,3′-diaminobenzidine and mounted with counter-staining.

For cell death, tissue sections were semi-quantitatively evaluated by a researcher blind to the treatment conditions using light microscopy (Leica). Brown-stained cells in the striatum, WM, and hippocampus were scored for each animal on both sides of the brain using Histolab software (Microvision Instrument). Results were expressed as mean number of positive brown cells ± SEM per field. Four sections for each field of interest were counted per brain (TUNEL: controls, $n = 4$; LPS group, $n = 8$; Caspase-3: controls, $n = 8$; LPS group, $n = 7$).

MBP and GFAP immunohistochemistry. Anti-mouse MBP and anti-mouse GFAP [monoclonal mouse antibodies, Chemicon International (Temecula, CA) and Sigma Chemical Co.] were used as primary antibodies for detection of myelin and astrocytes. Sections were fixed for 3 min in methanol, 4 min in acetone, and dried for 30 min. After rinsing with PBS [without calcium and magnesium 1× (Invitrogen), 2% gelatin and 0.25% Triton], brain sections were incubated with primary antibody diluted at 1:1000 in PBS overnight. Sections were rinsed in PBS and incubated with biotinylated anti-mouse IgG diluted at 1:200 in PBS for 90 min. Sections were rinsed in PBS and incubated with streptavidin-biotin-peroxidase complex (Amersham Biosciences AB, Uppsala, Sweden) diluted at 1:400 in PBS for 90 min. After rinsing once in PBS and once in Tris 50 mM, the reaction was visualized with 3.3′-diaminobenzidine and mounted with counter-staining. For MBP study, we used a semi-quantitative method to study the intensity of labeling. Each animal was classified in a group according the staining observed, *i.e.* +++ for half the field stained, ++ for a quarter of the field stained, + for less than a quarter, and 0 for no staining.

Statistics. Quantitative data were expressed as mean values ± SEM for each group and results were analyzed using the *t* test. The χ^2 test was used for semi-quantitative MBP staining. The significance level was set at $p < 0.05$.

RESULTS

Physiologic parameters. We observed a significant difference in changes in weight in pregnant rats between G19 and G20 after the first LPS injection, as the LPS group lost weight whereas controls gained weight (LPS group, $n = 15$, -6.31 ± 2.60 g *versus* controls, $n = 10$, 9.70 ± 4.94 g; $p < 0.01$). We did not observe any difference in the dropping stage in the LPS group compared with controls (LPS group, 21.23 ± 0.11 d *versus* controls, 21.35 ± 0.15) nor in the number of live newborns per litter (LPS group, 9 ± 0.81 *versus* controls, 11 ± 1.01). However, significant differences were observed in both body and brain weights in the LPS group compared with controls at P1 and P7 (Table 2). Significant decreases (30%, $p < 0.01$, and 20%, $p < 0.01$) in body weight was measured in the LPS group compared with controls at P1 and P7, respectively. A significant loss of brain weight in the LPS group compared with controls was also observed at P1 (–15%, $p < 0.01$) and P7 (–16%, $p < 0.01$).

Quantification of cytokine mRNA by RT-QPCR. Considering that the difference in the threshold cycle of the two replicates should be <0.5 to be useful, the results from several animals were not used for this experiment. No difference was seen at P1 for IL-6 between LPS and control groups (data not shown). At P1 (Fig. 1*A*), a slight nonsignificant (18%) decrease in TNF-α mRNA expression (0.82-fold change in gene expression in LPS group compared with controls; ΔC_T: LPS group, $n = 14$, 14.56 ± 0.15 *versus* controls, $n = 13$, 14.19 ± 0.16) and a significant (64%) increase in IL-1β mRNA expression (1.64-fold change in gene expression in LPS group compared with controls; ΔC_T: LPS group, $n = 14$, 15.06 ± 0.16 *versus* controls, $n = 8$, 15.66 ± 0.13, $p < 0.05$) were observed. At P7 (Fig. 1*B*), a significant (37%) decrease was observed in TNF-α mRNA expression (0.63-fold change in gene expression in LPS group compared with controls; ΔC_T: LPS group, $n = 6$, 14.34 ± 0.21 *versus* controls, $n = 7$, 13.59 ± 0.09, $p < 0.01$) whereas IL-1β expression was similar to controls (1.03-fold change in gene expression in LPS group compared with controls; ΔC_T: LPS group, $n = 10$, 16.41 ± 0.27 *versus* controls, $n = 5$, 16.33 ± 0.35).

Cresyl violet staining. No cystic lesions were observed in the LPS group at P1 and at P7 (data not shown).

Cell death study: caspase-3 and TUNEL. A significant (91%) increase was observed in the number of caspase-3–positive cells per field in the subventricular striatal zone (Fig. 2, LPS group: 40 ± 5 *versus* controls: 21 ± 6 cells, $p < 0.05$), whereas a nonsignificant (30%) increase was observed in the WM external capsule zone (LPS group: 30 ± 4 *versus* controls: 23 ± 4) at P1. At P7 (Fig. 3 and Fig. 4), a significant increase in cell death was observed in the periventricular zone. A 114% increase in the number of caspase-3–positive cells per field was measured in the periventricular striatum (LPS group: 18 ± 2 *versus* controls: 8 ± 1, $p < 0.01$), a 177% increase in the periventricular WM at the level of the external capsule (LPS group: 12 ± 3 *versus* controls: 4 ± 1, $p < 0.05$) and a 133% increase in the germinative ventricular zone (LPS group: 22 ± 4 *versus* controls: 9 ± 2, $p < 0.05$).

We also observed a significant (76%) increase in TUNEL-positive cells per field at P7 in the periventricular striatum (LPS group: 24 ± 3 *versus* controls: 14 ± 2, $p < 0.05$; Fig. 5), whereas nonsignificant (26% and 21%) increases were observed in the periventricular WM (LPS group: 9 ± 1 *versus* controls: 7 ± 1) and germinative ventricular zone (LPS group: 59 ± 5 *versus* controls: 49 ± 3), respectively.

Myelination study: MBP immunochemistry. We observed significant hypomyelination in the LPS group compared with controls in both the external (Khi2, ddl = 3, $p < 0.01$) and internal capsule (Khi2, ddl = 3, $p < 0.05$) (Fig. 6 and Table 3).

Astrocyte structure: GFAP immunohistochemistry. Typical astrogliosis was observed in fimbria hippocampus and WM both in the internal and external capsule at P7 in the LPS group (Fig. 7).

Table 2. *Comparison of body and brain weights at P1 and P7*

		Body weight (g)	Brain weight (g)
P1	Controls ($n = 24$)	7.73 ± 0.19	0.27 ± 0.01
	LPS group ($n = 36$)	5.39 ± 0.12**	0.23 ± 0.01**
P7	Controls ($n = 16$)	19.6 ± 0.56	0.73 ± 0.01
	LPS group ($n = 27$)	15.55 ± 0.43**	0.62 ± 0.01**

We noticed a significant decrease of body weight in the LPS group compared with controls at P1 (–30%) and P7 (–20%). We also observed a significant loss of brain weight at P1 (–15%) and P7 (–16%) in the LPS group compared with controls. Results are expressed as mean ± SEM. Comparisons with controls were performed using the *t* test (**$p < 0.01$)

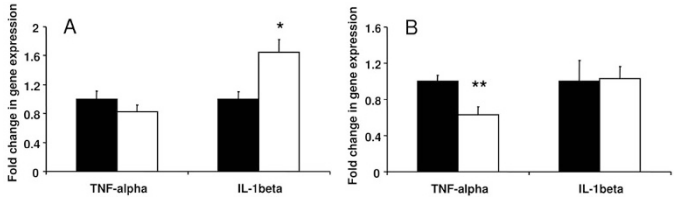

Figure 1. Variations in expression of TNF-α and IL-1β at P1 (*A*) and P7 (*B*). At P1, for TNF-α, $n = 13$ for controls (*black bars*) and $n = 14$ for LPS group (*white bars*) and for IL-1β, $n = 8$ for controls and $n = 14$ for LPS group. At P7, for TNF-α, $n = 7$ for controls and $n = 6$ for LPS group and for IL-1β, $n = 5$ for controls and $n = 10$ for LPS group. Results are expressed as mean ± SEM. Comparisons with controls were performed using *t* test (*$p < 0.05$ and **$p < 0.01$).

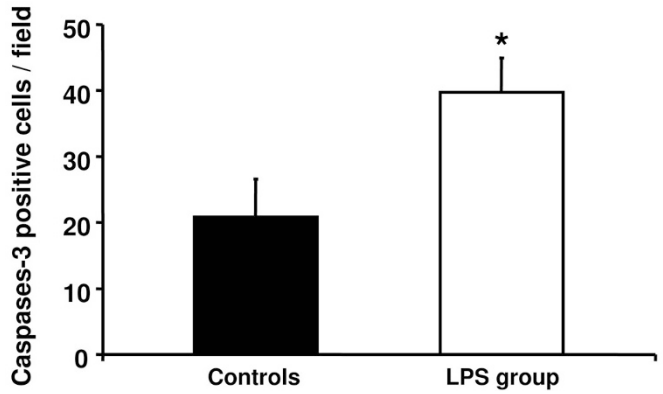

Figure 2. Number of caspase-3–positive cells per field in the subventricular striatal zone at P1 (controls, $n = 8$; LPS group, $n = 7$). Comparisons with controls were performed using *t* test (*$p < 0.05$).

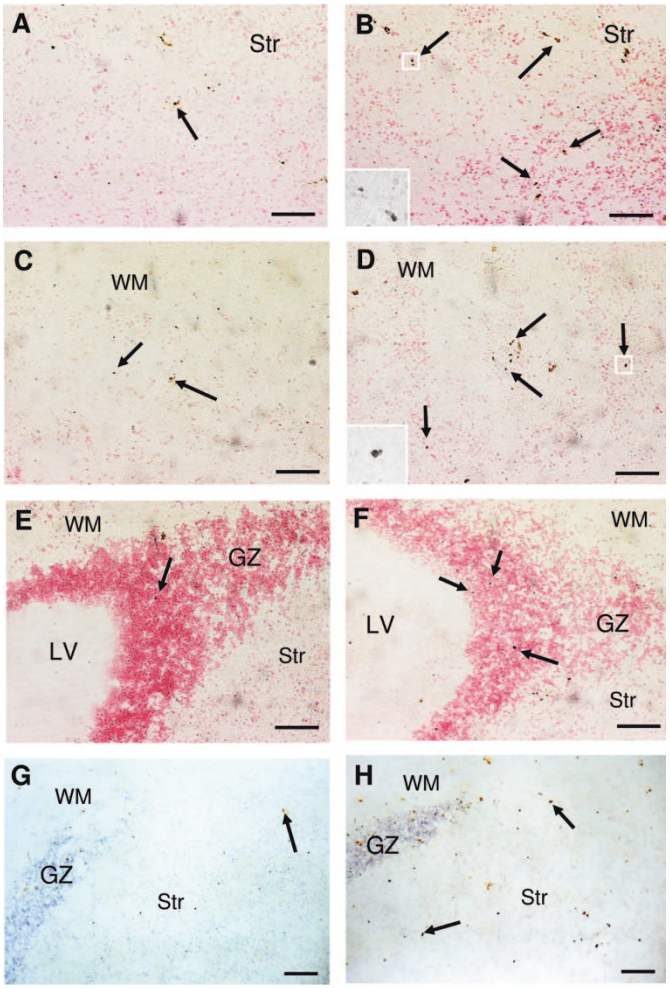

Figure 3. Cell death in rat brains at P7. Labeled cells with caspase-3 immunohistochemistry (*A–F*) and TUNEL (*G* and *H*), showing apoptotic cells in periventricular striatum (*Str*) (*A, B, G,* and *H*) in periventricular WM (*C* and *D*), and in germinative zone (*GZ*) (*E* and *F*). Inserts in *B* and *D* are the magnified part of the white boxes. TUNEL: controls, $n = 4$; LPS group, $n = 8$; Caspase-3: controls, $n = 8$; LPS group, $n = 7$. *A, C, E,* and *G* are control sections. Bar = 100 μm.

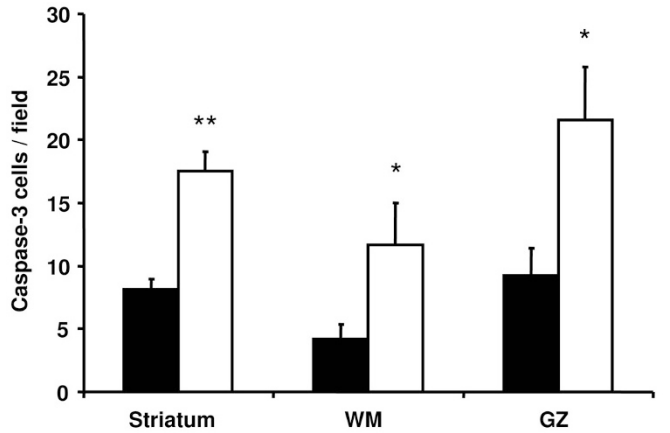

Figure 4. Number of caspase-3 apoptotic cells per field at P7 in periventricular striatum, periventricular WM, and germinative ventricular zone. Controls (*black bars*), $n = 8$; LPS group (*white bars*), $n = 7$. Results are expressed as mean ± SEM. Comparisons with controls were performed using *t* test (*$p < 0.05$ and **$p < 0.01$).

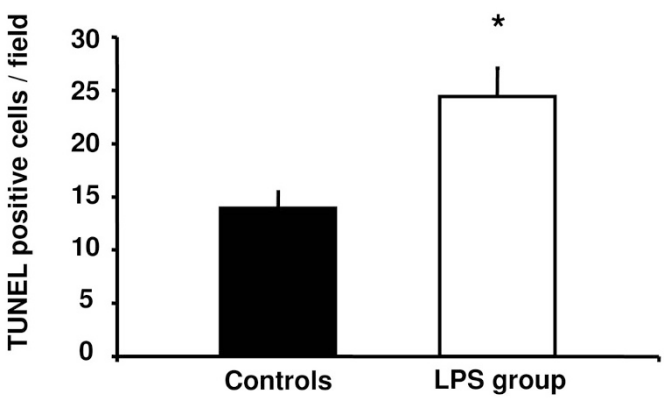

Figure 5. Number of apoptotic cells per field labeled with TUNEL in periventricular striatum, at P7 (controls, $n = 4$; LPS group, $n = 8$). Results are expressed as mean ± SEM. Comparisons with controls were performed using *t* test (*$p < 0.05$).

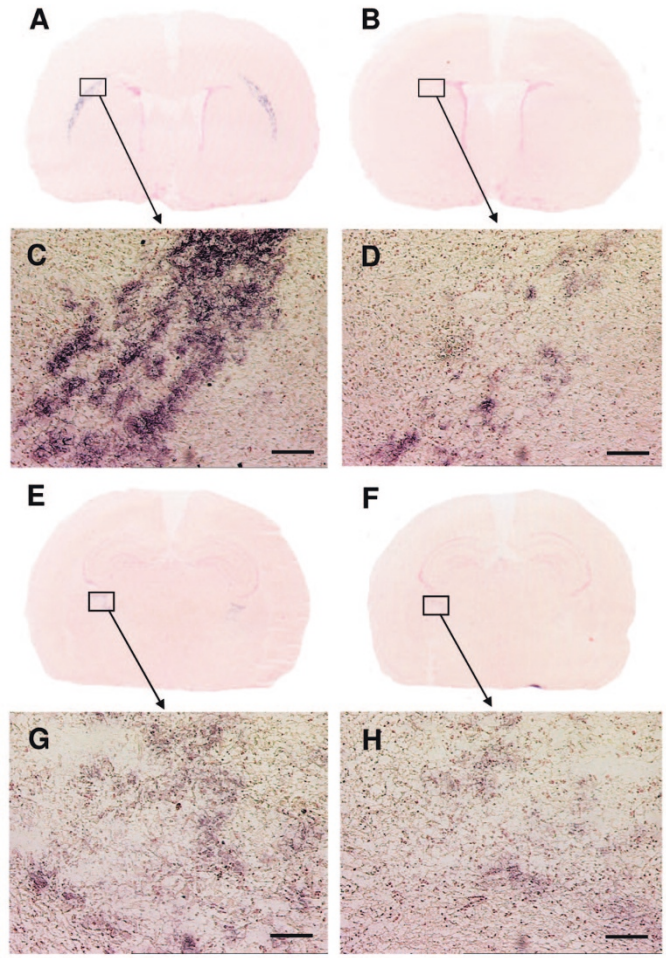

Figure 6. Labeled sections with MBP immunohistochemistry at P7 (controls, $n = 8$; LPS group, $n = 8$). Normal myelination was noted in control brains (*A, C, E,* and *G*), whereas hypomyelination or lack of myelination occurred in LPS group brains (*B, D, F,* and *H*). Bar = 100 μm.

DISCUSSION

We demonstrated here that LPS administration in pregnant rats at G19 and G20 induced multisite WM injury in P1 and P7 progeny, characterized by astrogliosis, apoptosis, and damage to myelination. The new major finding of this study was

Table 3. *Number of animals in each group according to the MBP staining*

		0	+	++	+++
External capsule	Controls ($n = 8$)	0	2	2	4
	LPS group ($n = 8$)	6	2	0	0
Internal capsule	Controls ($n = 7$)	1	1	2	3
	LPS group ($n = 8$)	6	2	0	0

We observed difference of distribution in LPS group compared with controls in both external and internal capsule. We noticed myelination in control brains, whereas we observed hypomyelination or lack of myelination in LPS group brains (MBP staining—0: no staining, +: less than a quarter of the field stained, ++: a quarter of the field stained, +++: half of the field stained).

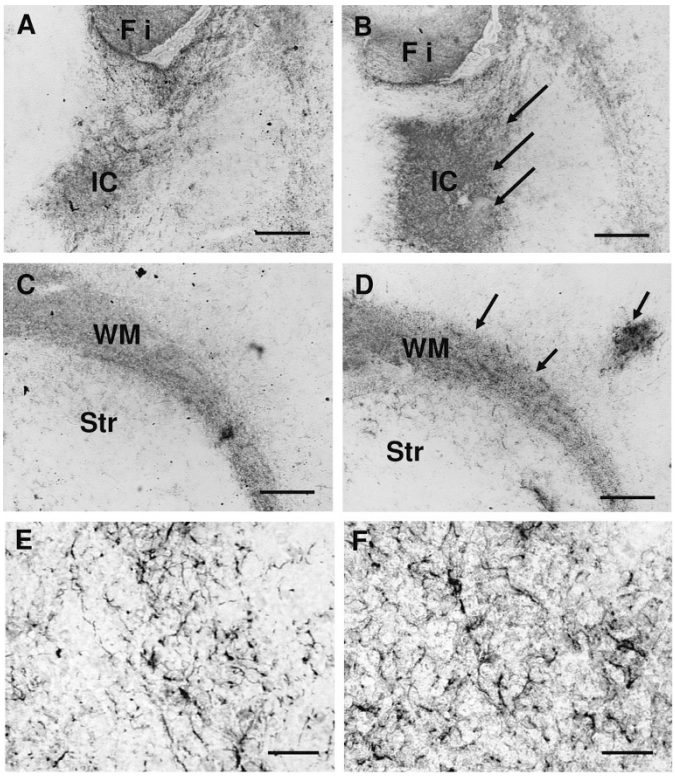

Figure 7. Labeled cells with GFAP immunohistochemistry at P7 in the internal (*IC*) (*A, B, E,* and *F*) and external capsule (*EC*) (*C* and *D*) (controls, $n = 8$; LPS group, $n = 8$). *A, C,* and *E* are control sections. Bar = 500 μm and 30 μm for *E* and *F*.

that LPS treatment induced hypomyelination in the WM, persistent PCD in the WM and deep gray matter, and a late inflammatory reaction.

Maternal LPS and neonatal brain cytokines. We found a significant increase in IL-1β expression in pup brains at P1 (3 d after the last maternal administration of LPS). An inflammatory reaction has already been described in a similar model; a high dose (4 mg/kg) administered at G18 induced peaks of expression of IL-1β and TNF-α in the fetal brain at 1 and 3 h postinjection (17). The persistent inflammatory reaction that we observed in pup brains is to our knowledge the first demonstration of prolonged increased expression of IL-1β.

Investigating cytokine immunoreactivity in human brains with PVL, Kadhim *et al.* (22) reported an inflammatory reaction with high levels of TNF-α and, to a lesser extent, IL-1β. A significant cerebral decrease in TNF-α occurred at P7 in the present study. These results are in contrast to others reporting an increase in TNF-α in the fetal rat brain a few hours after maternal LPS administration at G18 and G19 (17) or at G15 (5), whereas a significant decrease in TNF-α was found in fetal brains after maternal LPS administration at G16 (23). The differences between these studies may be due to different gestational ages at exposure, species and strains, dose and quality of LPS, and fetal environment (24).

A number of ways in which cytokines cause fetal brain injury have been proposed. They are able to affect the blood-brain barrier permeability (25) and may indirectly cause astrogliosis and damage to brain tissue through stimulation of NO and associated free radicals (26). IL-1β, a pleiotropic cytokine with multiple biologic actions, can be produced in the CNS from microglia, astrocytes, and neurons. *In vitro,* it regulates survival of fetal neurons, inhibits proliferation of oligodendrocyte progenitors, and activates astrocytes (27). Direct intra-cerebral and systemic injection of IL-1β have been reported to stimulate astrogliosis and angiogenesis in the developing rodent brain (28).

PCD in the periventricular white and deep gray matter. Apoptosis has been reported to be a contributing mechanism for cell death in infants with WM injury (29). As previously demonstrated in pregnant rabbits and guinea pigs, *E. coli* inoculation into the uterine horns or into the cervix resulted in abundant PCD in the WM 2 d later (16,30). Active caspase-3 is initially low in the developing rat brain, but rises rapidly in the prenatal and early postnatal period to a peak and then declines (31). In our study, we observed a significant increase in caspase-3 cells in the periventricular WM and striatum. Observed first at P1, this multisite cell death was still present at P7.

Proinflammatory cytokines may cause brain injury through different mechanisms including apoptosis (32). In a model of intracerebral LPS injection, co-administration of LPS with IL-1 receptor antagonist significantly reduced increases in caspase-3 activity in the neonatal rat brain whereas TNF-α antibody had no effects (33). In cell culture, IL-1β has been linked directly with caspase-3 activation following hypoxic injury *via* NO (34).

Different authors have suggested that the myelination disorders of WM injury result from cell death of oligodendrocyte progenitors mediated partially by cytokines (7,35). In several models of hypoxia-ischemia, it has been reported that death of oligodendrocyte progenitors is due to the caspase-mediated mechanisms of apoptosis (36).

Maternofetal inflammation and WM injury. Patients with cystic PVL develop neuronal dysfunction, far beyond WM lesions, resulting in mental retardation or extrapyramidal symptoms. Recent MRI studies have shown that premature infants at term have significant reduction in volume of cerebral cortical and deep nuclear gray matter in comparison with term-born infants. The pattern of cerebral changes was related most significantly to the degree of immaturity at birth and was concomitant with WM injury (37).

We observed astrogliosis with hypertrophic astrocytes in the internal and external capsules, with significantly reduced

MBP staining. Diffuse spread of abnormal astrocytes in WM is considered to be a variant of WM damage in neonates. Such lesions may be accompanied by myelination abnormalities, secondary cyst formation, and ventricular enlargement. The injured cell types that provoke this gliosis are believed to be oligodendrocyte progenitors because the distribution of such lesions is similar to regions of myelination disorders. Evidence from clinical studies that reduced myelination and oligodendrocytes are observed concomitantly with WM injury in the infant brain supports the possibility that the maturation of myelin-forming oligodendrocytes is disrupted (38). Other potential mechanisms of injury include activation of microglia and axonal damage (39).

The internal capsule consists of a massive WM pathway linking the cerebral cortex with other parts of the brain. In infants with cerebral palsy (40), MRI studies have demonstrated that abnormal signal intensity in the internal capsule is an accurate predictor of neurodevelopmental outcome. It will be interesting to explore axonal damage further in our rat model, and to establish whether motor dysfunction occurs later on.

Anorexia is a well-known effect of LPS in rats. Fetal undernutrition has been implicated in myelination disorders and reduction in brain total volume (41). We observed restricted fetal growth in P1 offspring without catch-up at P7. This was associated with maternal weight loss after LPS treatment. This may be an aggravating factor of the hypomyelination observed in our model.

In conclusion, our experimental model of maternal inflammation causes late IL-1β responses in pup brains associated with significant WM lesions such as cell death, hypomyelination and astrogliosis in newborn rats. Since this cytokine may play a role in the development of brain injuries in neonates, investigating the mechanisms of cell damage and death may help the understanding of these processes in infants.

Acknowledgments. The authors thank L. Schwenndimann and P. Olivier for technical assistance.

REFERENCES

1. Volpe JJ 2001 Neurobiology of periventricular leukomalacia in the premature infant. Pediatr Res 50:553–562
2. Perlman JM 1998 White matter injury in the preterm infant: an important determination of abnormal neurodevelopment outcome. Early Hum Dev 53:99–120
3. Dammann O, Leviton A 1997 Maternal intrauterine infection, cytokines and brain damage in the preterm newborn. Pediatr Res 42:1–8
4. Back SA, Rivkees SA 2004 Emerging concepts in periventricular white matter injury. Semin Perinatol 28:405–414
5. Bell MJ, Hallenbeck JM, Gallo V 2004 Determining the fetal inflammatory response in an experimental model of intrauterine inflammation in rats. Pediatr Res 56:541–546
6. Leviton A, Gilles F 1996 Ventriculomegaly, delayed myelination, white matter hypoplasia and "periventricular" leukomalacia: how are they related? Pediatr Neurol 15:127–136
7. Back SA, Volpe JJ 1997 Cellular and molecular pathogenesis of periventricular white matter injury. MRDD Res Rev 3:96–107
8. Dammann O, Leviton A 2000 Role of the fetus in perinatal infection and neonatal brain damage. Curr Opin Pediatr 12:99–104
9. Rothwell NJ, Luheshi GN 2000 Interleukin 1 in the brain: biology, pathology and therapeutic target. Trends Neurosci 23:618–625
10. Yoon BH, Jun JK, Romero R, Park KH, Gomez R, Choi JH, Kim IO 1997 Amniotic fluid inflammatory cytokines (interleukin-6, interleukin-1beta and tumor necrosis factor-alpha), neonatal brain white matter lesions, and cerebral palsy. Am J Obstet Gynecol 177:19–26
11. Ellison VJ, Mocatta TJ, Winterbourn CC, Darlow BA, Volpe JJ, Inder TE 2005 The relationship of CSF and plasma cytokine levels to cerebral white matter injury in the premature newborn. Pediatr Res 57:282–286
12. Saliba E, Henrot A 2001 Inflammatory mediators and neonatal brain damage. Biol Neonate 79:224–227
13. Fiuza C, Suffredini AF 2001 Human models of innate immunity: local and systemic inflammatory responses. J Endotoxin Res 7:385–388
14. Young RS, Yagel SK, Towfighi J 1983 Systemic and neuropathologic effects of *E. coli* endotoxin in neonatal dogs. Pediatr Res 17:349–353
15. Buttini M, Boddeke H 1995 Peripheral lipopolysaccharide stimulation induces interleukin-1β messenger RNA in rat brain microglial cells. Neuroscience 65:2:523–530
16. Debillon T, Gras-Leguen C, Vérielle V, Winer N, Caillon J, Rozé JC, Gressens P 2000 Intrauterine infection induces programmed cell death in rabbit periventricular white matter. Pediatr Res 47:736–742
17. Cai Z, Pan ZL, Pang Y, Evans OB, Rhodes PG 2000 Cytokine induction in fetal rat brains and brain injury in neonatal rats after maternal lipopolysaccharide administration. Pediatr Res 47:64–72
18. Clancy B, Darlington RB, Finlay BL 2001 Translating developmental time across mammalian species. Neuroscience 105:7–17
19. Altman J, Bayer SA 1995 Atlas of Prenatal Rat Brain Development. CRC Press, Boca Raton, FL
20. Paxinos G, Watson G 1986 The Rat Brain in Stereotaxic Coordinates. Academic Press, Orlando, FL
21. Livak KJ, Schmittgen TD 2001 Analysis of relative gene expression data using real-time quantitative PCR and the $2^{-\Delta\Delta CT}$ Method. Methods 25:402–408
22. Kadhim H, Tabarki B, Verellen G, De Prez C, Rona AM, Sebire G 2001 Inflammatory cytokines in the pathogenesis of periventricular leukomalacia. Neurology 56:1278–1284
23. Urakubo A, Jarskog LF, Lieberman JA, Gilmore JH 2001 Prenatal exposure to maternal infection alters cytokines expression in the placenta, amniotic fluid and fetal brain. Schizophr Res 47:27–36
24. Hagberg H, Mallard C 2005 Effect of inflammation on central nervous system development and vulnerability. Curr Opin Neurol 18:117–123
25. Saija A, Princi P, Lanza M, Scalese M, Aramnejad E, De Sarro A 1995 Systemic cytokine administration can affect blood-brain barrier permeability in the rat. Life Sci 56:775–784
26. Balasingam V, Tejada-Berges T, Wright E, Bouckova R, Yong VW 1994 Reactive astrogliosis in the neonatal mouse brain and its modulation by cytokines. J Neurosci 14:846–856
27. Basu A, Krady JK, Levison SW 2004 Interleukin 1: a master regulator of neuroinflammation. J Neurosci Res 78:151–156
28. Cai Z, Lin S, Pang Y, and Rhodes PG 2004 Brain injury induced by intracerebral injection of interleukin-1beta and tumor necrosis factor-alpha in the neonatal rat. Pediatr Res 56:377–384
29. Chamnanvanakij S, Margraf LR, Burns D, Perlman JM 2002 Apoptosis and white matter injury in preterm infants. Pediatr Dev Pathol 5:184–189
30. Patrick LA, Gaudet LM, Farley AE, Rossiter JP, Tomalty LL, Smith GN 2004 Development of a guinea pig model of chorioamnionitis and fetal brain injury. Am J Obstet Gynecol 191:1205–1211
31. Mooney SM, Miller MW 2000 Expression of bcl-2, bax and caspase-3 in the brain of the developing rat. Brain Res Dev Brain Res 123:103–117
32. Selmaj K, Raine CS, Farooq M, Norton WT, Brosnan CF 1991 Cytokine cytotoxicity against oligodendrocytes. Apoptosis induced by lymphotoxin. J Immunol 147:1522–1529
33. Cai Z, Pang Y, Lin S, Rhodes PG 2003 Differential roles of tumor necrosis factor-α and interleukin-1β in lipopolysaccharide-induced brain injury in the neonatal rat. Brain Res 975:37–47
34. Hu S, Peterson PK, Chao CC 1997 Cytokine-mediated neuronal apoptosis. Neurochem Int 30:427–431
35. Rezaie P, Dean A 2002 Periventricular leukomalacia, inflammation and white matter lesions within the developing nervous system. Neuropathology 22:106–132
36. Ness JK, Romanko MJ, Rothstein RP, Wood TL, Levison SW 2001 Perinatal hypoxia-ischemia induces apoptotic and excitotoxic death of periventricular white matter oligodendrocyte progenitors. Dev Neurosci 23:203–208
37. Inder TE, Warfield SK, Wang H, Huppi PS, Volpe JJ 2005 Abnormal cerebral structure is present at term in premature infants. Pediatrics 115:286–294
38. Iida K, Takashima S, Ueda K 1995 Immunohistochemical study of myelination and oligodendrocyte in infants with periventricular leukomalacia. Pediatr Neurol 13:296–304
39. Back SA, Han BH, Luo NL, Chricton CA, Xanthoudakis S, Tam J, Arvin KL, Holtzman DM 2002 Selective vulnerability of late oligodendrocyte progenitors to hypoxy-ischemia. J Neurosci 22:455–463
40. Stewart RM 1942 Observations on the pathology of cerebral diplegia. Proc R Soc Med 36:25–32
41. Exton MS, Bull DF, King MG 1995 Behavioral conditioning of lipopolysaccharide-induced anorexia. Physiol Behav 57:401–405